Resonance coupling in plasmonic nanomatryoshka homo- and heterodimers

Arash Ahmadivand,[a] Raju Sinha, and Nezih Pala
Department of Electrical and Computer Engineering, Florida International University, 10555 W Flagler St., Miami, Florida 33174, USA

(Received 23 March 2016; accepted 24 May 2016; published online 1 June 2016)

Here, we examine the electromagnetic (EM) energy coupling and hybridization of plasmon resonances between closely spaced concentric nanoshells known as "nanomatryoshka" (NM) units in symmetric and antisymmetric compositions using the Finite Difference Time Domain (FDTD) analysis. Utilizing plasmon hybridization model, we calculated the energy level diagrams and verified that, in the symmetric dimer (in-phase mode in a homodimer), plasmonic bonding modes are dominant and tunable within the considered bandwidth. In contrast, in the antisymmetric dimer (out-of-phase mode in a heterodimer), due to the lack of the geometrical symmetry, new antibonding modes appear in the extinction profile, and this condition gives rise to repeal of dipolar field coupling. We also studied the extinction spectra and positions of the antibonding and bonding modes excited due to the energy coupling between silver and gold NM units in a heterodimer structure. Our analysis suggest abnormal shifts in the higher energy modes. We propose a method to analyze the behavior of multilayer concentric nanoshell particles in an antisymmetric orientation employing full dielectric function calculations and the Drude model based on interband transitions in metallic components. This study provides a method to predict the behavior of the higher energy plasmon resonant modes in entirely antisymmetric structures such as compositional heterodimers.
[http://dx.doi.org/10.1063/1.4953351]

I. INTRODUCTION

The optical characteristics of noble metallic structures in nanoscale dimensions have been described by localized surface plasmon resonances (LSPRs), which correspond to free electron coherent oscillations in the conduction band when illuminated by an incident light at the optical frequencies.[1] Metallic nanostructures with subwavelength dimensions have been extensively employed in the design and fabrication of integrated nanoplasmonic structures and devices for numerous applications such as biological and chemical sensing,[2] and surface-enhanced Raman spectroscopy (SERS).[3] Studies have strongly proved that various parameters such as shape, geometrical dimensions, chemical composition, and optical characteristics of the nanostructures have a significant impact on intensity, position, and frequency of the plasmon resonant modes.[4,5] In addition, the behavior of plasmon resonances strongly depends on the existence of an adjacent individual nanoparticle. Subtle variations in the elucidated chemical, physical, and optical properties influence the plasmon resonance condition due to the near-field coupling of dipoles, quadrupoles, and higher-order poles under the excitation of an incident beam.[6] Coupling of plasmon resonances to proximal nanoparticles facilitates an opportunity to adjust the intensity of the LSPR at the desired spectrum via red- or blue-shifts. Moreover, by changing the distance between nanoparticles, scattering cross-section spectra can be tuned, which can be exploited for imaging and sensing purposes.[7]

[a]Corresponding Author: aahma011@fiu.edu

Individual modifications in the structural and environmental parameters of a given nanostructure influence the precision of LSPR sensing significantly.[8] To improve the quality of designed plasmonic devices, all alterations must be performed correctly and accurately. For instance, it is well accepted that increments in the refractive index of the local environment cause red-shift of the plasmon resonance frequency to the longer wavelength spectra.[9] More studies have also shown that this sensitivity of the plasmon resonance frequency can be improved by changing the shape and size of the nanoparticles simultaneously in the correct manner.[8,9] Considering the dipolar coupling,[1,10] and Drude model,[1] the nanoparticle geometry-dependent factor (shape factor) as κ, and the refractive index of host substance by n_h, we can describe the precise surface plasmon wavelength as:

$$\lambda_{SP} = \sqrt{\frac{\varepsilon_0 m_e(\varepsilon_\infty + \kappa n_h^2)}{Ne^2}} \tag{1}$$

where, N is the electron density of the employed metal, ε_0 and ε_∞ are the permittivity of free space and high-frequency response respectively, and m_e is the effective electron mass. The equation above indicates that increasing the refractive index of the surrounding medium and the shape factor directly increases the size of the LSPR movement (red-shift to the longer wavelengths), and Parshant *et al.*[9] have proved that this modification raises the sensitivity and accuracy of plasmon resonance coupling and sensing. Earlier computational results verified that nanoparticles with complex geometrical configurations show larger shape factors due to the number of tunable parameters in their structural geometry. For example, a simple sphere with a radius of r<50nm has a shape factor of approximately κ~2,[9] and for a simple nanoshell with the overall size of <50nm, the shape factor is κ ~3.1.[10] Hence, for a given structure and combination of nanoparticles, increasing complexity could help achieve larger red-shifts of LSPR to the near infrared spectrum and also more accurate sensing ability.

Two proximal nanoparticles (Ψ_1,Ψ_2) that are located in close proximity to each other are recognized as a two-member dimer configuration, which provides a significant EM field enhancement and localization of plasmon resonances at the coupling region (the offset gap distance between nanoparticles). Recently, dimers have attracted great attention for use in ultra-sensitive detectors and nanostructures, as well as SERS applications.[10–13] Several nanoparticles with different shapes and sizes in a symmetric configuration (the center of both particles is in the same axis and completely similar in structural and chemical properties leading to in-phase plasmon modes ($\Psi_1 + \Psi_2$)), have been discussed and studied previously.[9–13] Homodimer nanoassembly reflect only a bonding plasmon resonance mode under longitudinal-polarized excitation, and the peak of the dipolar mode appears in the gap between nanoparticles. Likewise, asymmetric dimer nanostructures (completely different particles with respect to the structural and chemical properties leading to out-of-phase plasmon modes (Ψ_1-Ψ_2)), of simple particles such as spheres and rods have been studied experimentally and theoretically for their energy levels and extinction cross-section properties.[14]

Illumination of two adjacent nanoparticles in a homodimer structure by an incident longitudinal-polarized light results in excitation of a bonding plasmon mode in the extinction diagram, which leads to a significant enhancement in the electric field at the coupling area, and consequently, a large red-shift of the plasmon resonance denoted by σ.[14,15] Additionally, reducing the offset gap between nanoparticles to a touching regime gives rise to a remarkable blue-shift of the LSPR to the shorter wavelengths, which is not considered for the proposed heterodimer structure in this study.[11] In contrast, in the heterodimer regime (out-of-phase mode), the adjacent heterodimer shows the antibonding modes as well as bonding modes resulting localized electric field enhancement at the outer sides of the dimer configurations and blue-shift of the plasmon resonance frequency, which is denoted by σ^*.[16] Both bonding and antibonding plasmon modes and their hybridized models are explained in the following sections. The plasmon response of the proposed nanostructures with expected red- and blue-shifts are also examined theoretically and numerically. Moreover, the effect of changes in the polarization direction and plasmon resonance reflection in both in-phase and out-of-phase plasmon modes are of interest for this study. Earlier works have shown that modifications in the polarization direction of an incident wave to the transverse polarized mode (perpendicular to the dimer axis) leads to an exactly opposite results in the shift of the plasmon

resonant modes and it is important to note that corresponding shifts of the LSPR are noticeably weaker than the former case.[16] In this limit, an antibonding mode is reported for the homodimer structure, while a bonding mode is observed for the heterodimer structure which are denoted by π and π^*, respectively.

In this work, we investigate the plasmon response and optical properties of plasmonic nanostructures composed of two concentric nanoshells that are placed in close proximity to each other and are known as NM dimers. The in-phase regime of NM dimer have already been studied by Prodan *et al*.[15] and the behavior of bonding modes are examined previously. In the antisymmetric regime, we show that the proposed dimer is able to support both bonding and antibonding plasmon modes, concurrently. Most of the previous investigations were limited to dimers with ordinary shapes or materials with similar compositions.[13–18] In this report, we extend our study to the NM structure with different metal compositions and sizes. This method allows us investigating the plasmon resonance behavior in symmetry-lacking structures. Moreover, we examine the quality of the plasmon resonance coupling in the NM structures with various geometrical dimensions to achieve enhanced and ultra-sensitive nanoplasmonic configurations.

II. CALCULATIONS AND THEORY

To investigate the behavior of the presented subwavelength dimer composed of NM structures, we used a three dimensional Finite-Difference Time-Domain (FDTD) method (Lumerical package). To this end, we used a model with spatial cell size dx=dy=dz=0.1 nm, with the number of cell units 12000, and perfectly matched layers (PMLs) for the boundary condition with 16 compacted layers with a high ratio of absorption of scattered fields. Moreover, by employing a linear plane wave as an incident light source, we excited surface plasmon resonances in the studied nanocomposition. For the analytical analysis, plasmon hybridization theory was used to calculate the extinction profiles of the dimer structure in symmetric and antisymmetric compositions.[15] Plasmonic nanoantennas that are located in closely-spaced regime support strong resonant modes with different energies and properties in the offset gap spot. Adjusting their size, material, and geometry, these plasmonic nanostructures can be tailored to sustain unique spectral lineshapes in the cross-sectional spectra such as Fano resonances characterized by a deep and narrow spectral windows.[19,20] Recently, methods such as multiparticle Mie theory,[21] and ab initio method,[22] have been used to analyze dipolar and multipolar electromagnetic field interference and spectral response of these structures. However, comparing various analytical methods, plasmon hybridization theory have been considered as a major and promising solution to characterize the plasmonic response of multiparticle structures.[15,23] The symmetry and antisymmetry of the entire structure play fundamental role in corresponding spectral response. It is well accepted that breaking the symmetry of nanoscale assemblies gives rise to formation of new antibonding modes across the plasmonic response.[24,25] To underlay the physical mechanism behind the formation of antibonding resonant modes, the dipolar momentum of bonding and antibonding modes can be compared. In complex nanoparticle assemblies, and in the nonretarded limit, the plasmonic antibonding mode does not have any net dipole momentum and cannot be coupled to the incident beam efficiently. On the other hand, in the retarded limit, antibonding mode becomes subradiant and bonding mode remains superradiant, therefore, any destructive interference between these modes gives rise to antisymmetric lineshapes on the extinction curve.[19–25]

III. RESULTS AND DISCUSSION

In this section, first, we examine the quality of bonding and antibonding plasmon resonance modes for a NM homodimer (symmetric ($\Psi_1 + \Psi_2$)) with the same geometrical parameters and metal compositions (gold) for both sides, while the separation or gap distance between NM units is approximately D_{in}~15 nm, which resembles the strong coupling regime and also the thickness of the rings is kept fix as 25 nm throughout the study. This examination helps us observe bonding and antibonding plasmon modes in heterostructures under illumination of incident polarized light.

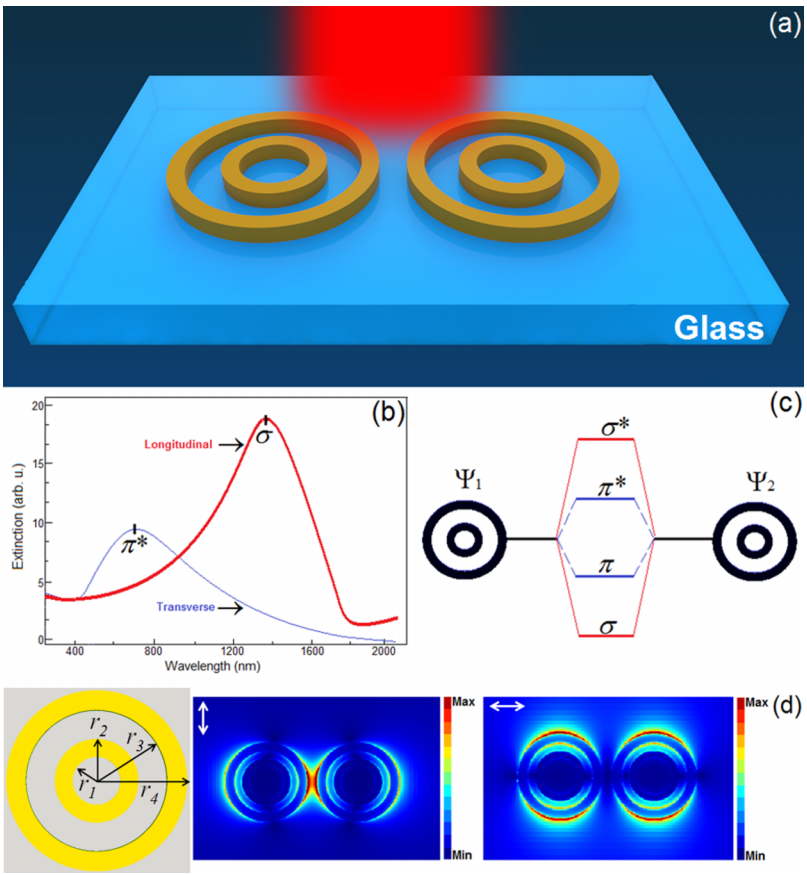

FIG. 1. (a) Schematic diagram of a gold NM homodimer ($\Psi_1 + \Psi_2$). **(b)** The extinction cross-section spectrum for both longitudinal (σ) and transverse (π^*) modes, which correspond to the bonding plasmon modes, according to the plasmon hybridization model. **(c)** Energy level diagram for plasmon hybridization homodimer in transverse and longitudinal polarizations excitations. **(d)** The E-field maps for the plasmon resonance excitation in the homodimer system under longitudinal and transverse polarized beams. The effective geometrical parameters (radii) which play a fundamental role in the investigation of the nanostructure and LSPR behavior, are also shown. These parameters are the same for both nanoparticles and are (r_1, r_2, r_3, r_4) = (60, 80, 105, 135) nm. The thickness for all cases is 25 nm.

Figure 1(a) shows a three-dimensional schematic picture of a symmetric homodimer, along with the geometrical parameters in the top-view picture (not to scale). It is already proved that the interaction of surface plasmon polaritons (SPPs) in the interior and exterior surfaces of a nanoshell can be described by the plasmon hybridization theory,[15,23] and the corresponding frequency for antisymmetric and symmetric modes can be specified by $|\omega_+\rangle$ and $|\omega_-\rangle$, respectively. Figure 1(b) illustrates the extinction cross-section profile for the observed plasmon resonant modes under excitation of longitudinal and transverse electric field polarization modes in strong coupling regime. Obviously, the two bonding plasmon modes result from the longitudinal (σ) (larger shift) and transverse (π^*) polarization modes with the extinction peaks at λ~1390nm and 780nm, respectively (see Fig. 1(c)). Figure 1(d) shows the plasmon resonance excitation as E-field maps for the homodimer antenna. One should note that these results have been predicted from the plasmon hybridization model for most of the comparable and simple homodimers with short red-shifts under the excitation by an incident longitudinally polarized light.[13,14] Considering the geometrical dimensions (r_1,r_2,r_3,r_4) = (60,80,105,135) nm for gold NM, we calculated the extinction spectra for the homodimer system in the strong interaction of the excited dipolar and multipolar fields (bonding modes only). Further, we evaluated the plasmon resonance behavior (coupling and shifting of the LSPR) during symmetry breaking for the NM dimer based on modifications in the geometrical sizes, while the chemical properties of the employed materials are the same in both sides. Accordingly, we modified

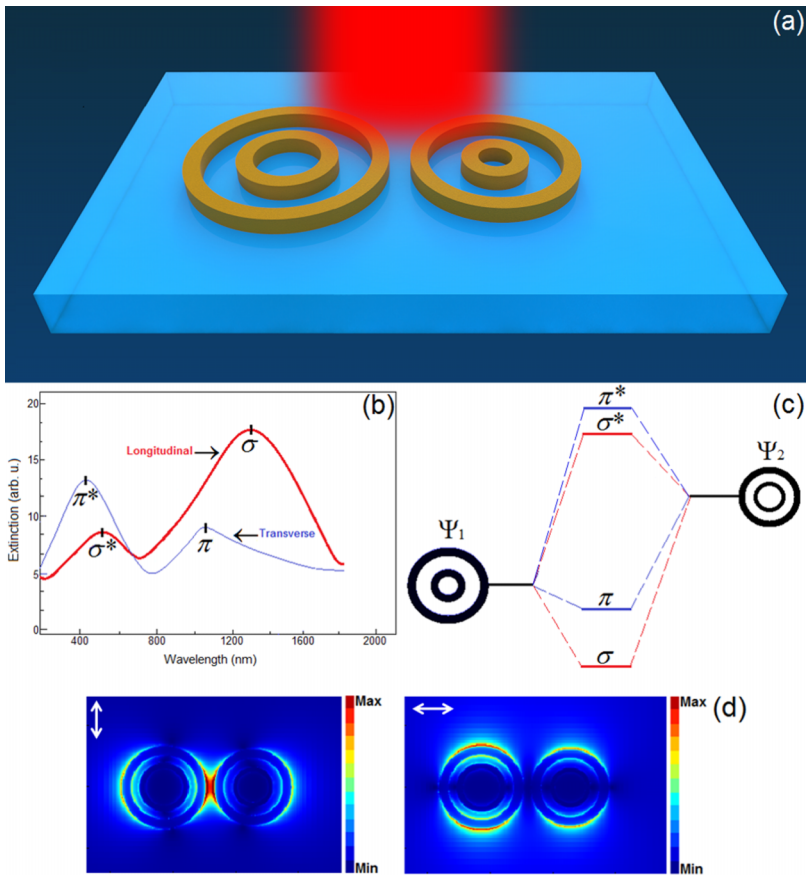

FIG. 2. **(a)** Schematic diagram of a gold antisymmetric dimer ($\Psi_1 + \Psi_2$) with the modified geometrical dimensions of (60, 80, 105, 135) nm for Ψ_1 and (50, 65, 95, 125) nm for Ψ_2. **(b)** The extinction cross-section spectra for both of the longitudinal and transverse polarization. The LSPR shows a trivial blue shift in the σ mode and also for the π^*-mode due to the coupling of plasmon modes. Hence, the extinction maximums are at λ~1360, 510 nm and 1080, 470 nm for (σ,σ^*) and (π,π^*), respectively. **(c)** Plasmon hybridization diagram for the proposed NM heterodimer in the transverse and longitudinal polarizations. **(d)** The E-field maps for the plasmon resonance excitation in the homodimer system under longitudinal and transverse polarized beams.

the radii of one of the gold NM units (Ψ_1) to (50,65,95,125) nm, while keeping the ones for the other (Ψ_2) at (60,80,105,135)nm (Heterodimer antenna, see Fig. 2(a)). The corresponding extinction cross-sectional profile is illustrated in Fig. 2(b), where two distinct extremes induced for each one of the incident polarized modes in the symmetry breaking regime. The incident longitudinal polarization excites the peaks at λ~1360nm (σ), 510nm (σ^*) while the incident transverse polarization results the extremes at λ~1080nm (π), 470nm (π^*) for bonding and antibonding plasmon modes in the antisymmetric regime (Ψ_1-Ψ_2), respectively. Utilizing the coupled dipole-dipole model and discrete approximation (DDA) method,[26,27] for the multipolar modes, we calculated the energy diagram for different regimes as shown in Fig. 2(c). It is shown that DDA method is a highly flexible analytical method for computing the spectral responses and corresponding extinction profiles of nanoscale structures.[28,29] Considering the proposed method in Ref. 27, therefore, the extinction cross-section for a NM unit can be written as:[28]

$$C_{ext} = \frac{4\pi k}{|E_0|^2} \sum_{i=1}^{2} \mathrm{Im}\left(E^*_{inc,j}.P_j\right) \tag{2}$$

where k is the wave vector, E_{inc} is the incident electric field, p is the dipole moment depending on the polarizability of NM unit and dipolar field. The polarizability and spectral response of a plasmonic NM is calculated and discussed in previous studies comprehensively.[30–32] Using

previously studied analysis, we extracted the plasmonic responses for both homo and heterodimers accurately. Considering the same chemical properties of plasmonic NM units, it is obvious that the antibonding mode as an abnormal mode repeals the excited dipoles of the small and large gold concentric nanoshells. These results encouraged us to develop a modified version of computations for analyzing the behavior of a dimer structure composed of two different NM units that will be discussed further. We plotted the E-field maps for the plasmon resonance hybridization in the gap spots between nanoparticle units for bonding modes (σ and π) positions in Fig. 2(d).

In the extinction cross-sectional diagrams, the compounds of the in-phase modes (σ and π^*) are significantly severe in comparison to the out-of-phase modes (σ^* and π) combinations. Therefore, the presented results based on the adapted simulation model for the NM heterodimer (asymmetric regime) are in the good agreement with the hybridization model.[15] Lassiter *et al.*[11] and Prodan *et al.*[15] have demonstrated that the extent of shifts in longitudinal polarization mode coupling is dramatically longer than the transverse ones (blue-shift), which is in agreement with our results and the plasmon hybridization model as well. The noteworthy feature of the studied plasmonic heterodimer is the noticeable red-shift of the LSPR to longer wavelengths, which is a significant shift in comparison with the behavior of analogous dimers composed of spherical compositions in the same simulation workplace (e.g. spheres, rods, and rings). This feature helps us to understand the sense of the plasmon energy shifts driven from the intense coupling of a gold NM dimer for bonding and antibonding plasmon resonant modes.

In continue, we present the influence of symmetry breaking on the optical response of the heterodimer structures with modifications in both chemical and physical characteristics. First, we used the previously used geometrical sizes of (60,80,105,135) nm for Ψ_1 and (50,65,95,125) nm for Ψ_2, but changed the metal of Ψ_2 to silver while keeping the Ψ_1 gold (see Fig. 3(a)). It is well accepted that individual silver nanoparticles show larger scattering spectra for an interacted light in comparison with the gold nanoparticles in the same condition,[33–35] and as a result, the corresponding sizes of gold unit must be larger than those for the silver unit in the NM heterodimer. This adjustment helps us provide an equal spectra of scattering for both sides to obtain corresponding extinction spectra. Illuminating the proposed silver-gold heterodimer by longitudinal and transverse polarization modes, we calculated the extinction cross-sectional diagram based on the DDA method with experimentally determined Palik constants (see Fig. 3(b)).[33] Considering the extinction profile in Fig. 3(b), we realized that bonding and antibonding extremes appear and noticeable red-shifts are observed for all of the observed modes (lower and higher energies). For the longitudinal polarization excitation, the maxima of bonding and antibonding modes (σ and σ^*) have been recorded around $\lambda \sim$1390nm and 700nm, respectively. In contrast, for the transverse modes, π and π^*-modes detected at $\lambda \sim$1090nm and 380nm, respectively. In this regime, plasmon resonance peak experienced a significant red-shift to the longer spectra under longitudinal polarization mode excitation. Figure 3(c) demonstrates how the bonding and antibonding extremes of plasmon hybridization model contributed to the examined heterostructure. In the position of the high-energy modes (σ^* and π^*), the size of the red-shift in the longitudinal polarization mode (σ^*) is larger than that in the π^*-mode. This condition verifies that the coupling strength in silver-gold NM heterodimer gives rise to a shift of the plasmon resonances to longer wavelengths in comparison with the isolated nanocomposition of silver shells. We also plotted corresponding E-field maps for the plasmon resonance confinement in the compositional dimer nanoantenna at the bonding mode wavelengths, as shown in Fig. 3(d). Herein, we observed a red-shift in the high energy modes of the incident longitudinal and transverse polarization modes, which caused by the presence of the silver shell unit on the other side of the dimer. Bachelier *et al.*[36] have verified that plasmon resonance shift in silver nanoparticles is in the direction of shorter wavelengths (blue-shift), however, this condition must be suppressed by coupling of the interband absorption of plasmon resonant modes in the gold nanoshells to the LSPR modes in the silver nanoshells. In addition, the interband transitions in the gold NM unit are prominent in the adjacent and above sections of the silver NM unit, and this situation leads to a strong coupling of interband transitions of gold particle to the silver plasmon resonances. A comparison of the coupling strength of the latest heterodimer and the homodimer structure with identical material and sizes shows the dominant behavior of the final structure.

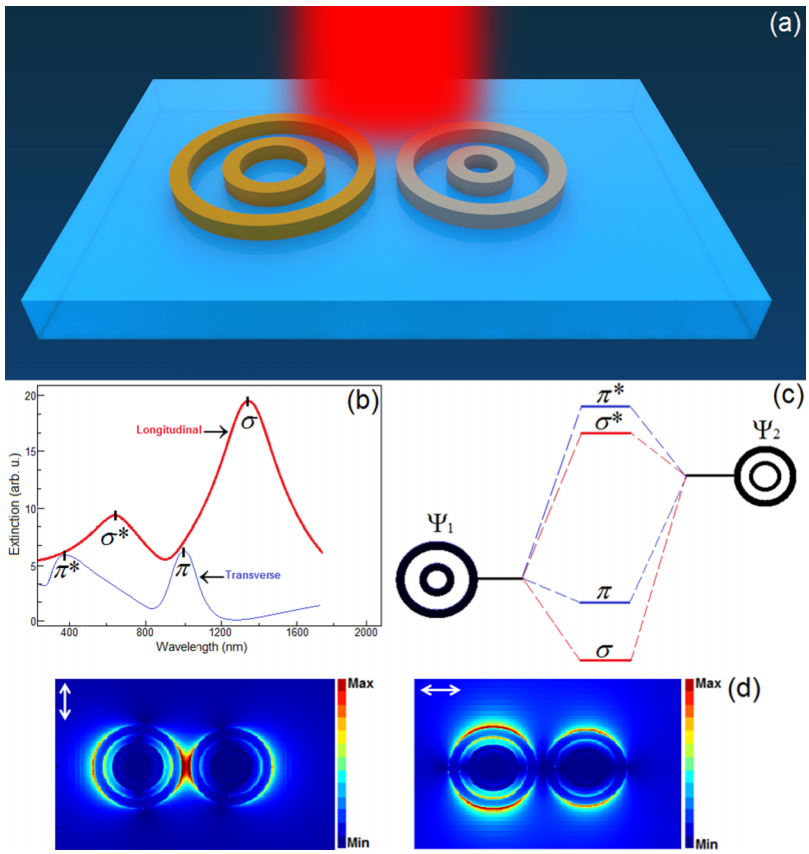

FIG. 3. **(a)** Schematic diagram of a silver-gold antisymmetric dimer with the modified geometrical dimensions, where gold system (Ψ_1) sizes are (60, 80, 105, 135) nm while the silver unit (Ψ_2) has the dimensions of (50, 65, 95, 125) nm. **(b)** The extinction cross-section spectrum variations for both of the incident polarized longitudinal and transverse plasmon modes. The LSPR shows a noticeable red-shift in σ^* and π^* modes due to the coupling of plasmon modes. The shift for the σ^*mode is larger than that of the π^* mode. **(c)** The standard plasmon hybridization model for the extinction spectra. **(d)** The E-field maps for the plasmon resonance excitation in the homodimer system under longitudinal and transverse polarized beams.

Further, we attempted to explain the mentioned deviation of the plasmon hybridization in the presented results, by employing full dielectric function in our calculations. To this end, we studied the feasible solutions to explain the observed abnormal red-shift in silver-gold nanoshells by the plasmon resonances due to the interband transitions in gold nanoshells. Considering the real and imaginary parts of refractive index of the interband contributions and the Drude model, one can estimate the corresponding spectra by using dielectric function calculations. Sheikholeslami *et al.*[14] have provided a method to explain the red-shift of LSPR in compositional nanosphere heterodimers based on a revision of the plasmon hybridization model in nanosphere investigations. Here, we further modified this method for a NM heterodimer in a quasi-approximation technique. In this method, plasmon resonance energy levels appear orderly for both transverse and longitudinal polarization modes, which includes the interband transitions in the gold NM and scattering of silver unit. Figure 3(c) exhibits the modified hybridization model for the silver-gold heterodimer. Due to the interband absorption of the optical power in the gold NM unit, we modified this model based on the material and orientation of the NM structures.

Ultimately, in order to calculate the coupling between NM units, we employed the modified hybridization model for plasmon resonance coupling, which contains the interband absorption of gold unit plus the scattering spectra (Figs. 3(c) and 4(a)). As we explained already, the interband absorption moved the plasmon resonance of the silver NM to the longer wavelengths (red-shift). Also, a comparison between the longitudinal plasmon antibonding mode (σ^*) for the heterodimer nanostructure and the transverse plasmon antibonding mode (π^*) indicates that the corresponding

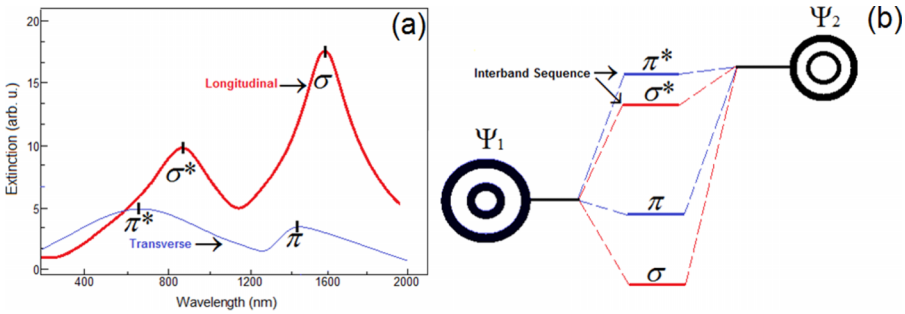

FIG. 4. Simulation results obtained using modified hybridization model for the same case presented in Fig. 3. **(a)** The extinction cross-section spectrum variations for both incident polarized longitudinal and transverse plasmon modes. As a result of our modified hybridization model, we correctly predicted the blue-shift for higher-energy modes and the red-shift of lower energies. Accordingly, the corresponded extremes of longitudinal plasmon resonance modes detected at λ~1600 and 900 nm for σ and σ* modes, and for transverse one occurred at λ~1450 and 540 nm for π and π* modes, respectively. **(b)** Modified plasmon hybridization diagram for NM heterodimer in the transverse and longitudinal polarizations.

coupling is purely of bonding form. Figure 4(b) demonstrates formation of the new bonding and the antibonding plasmon resonant modes in the revised hybridization model in which the upper levels designate the interband absorption spectra. The figure contains the anticipated interband absorption of gold and plasmon resonance of silver shells as well.

IV. CONCLUSIONS

In this study, we have examined the plasmon resonance coupling quality between NM units in an individual dimer structure using numerical analysis. Illuminating a symmetric dimer composed of gold NM with longitudinal- and transverse-polarized beams, we demonstrated the spectral response of the structure numerically. Then, breaking the symmetry of the dimer structure by changing the structural dimensions and choosing the same metal for both units, we observed bonding (σ and π) and antibonding (σ^* and π^*) plasmon modes for both of the incident polarized spectra. In this regime, we also observed a minor blue-shift in the bonding mode due to the symmetry breaking which is in complete agreement with the plasmon hybridization model. Finally, making changes in the physical dimensions and chemical compositions (silver-gold) of the utilized NM units showed a plasmon coupling and an interband absorption corresponding to the gold nanoshells. This led to an abnormal red-shift of higher energy modes (σ^* and π^*), which caused by coupling between interband absorption of gold shells and plasmon resonance of silver shells. Such a shift of LSPR is not expected by the plasmon hybridization model. Utilizing a modified hybridization model based on full dielectric function computations and the Drude model which have previously used for nanospheres and extended to multilayer shells, we obtained an expected blue-shift of plasmon resonance for higher energies. The variation of the optical response and plasmon resonance which caused by subtle structural and compositional alterations could transmute the modified nanostructures into a multipurpose scheme for LSPR sensing applications.

ACKNOWLEDGEMENT

This work is supported by NSF CAREER program with the Award number: 0955013, and by Army Research Laboratory (ARL) Multiscale Multidisciplinary Modeling of Electronic Materials (MSME) Collaborative Research Alliance (CRA) (Grant No. W911NF-12-2-0023, Program Manager: Dr. Meredith L. Reed). Raju Sinha gratefully acknowledges the financial support provided through presidential fellowship by the University Graduate School (UGS) at Florida International University.

[1] U. Kreibig and M. Vollmer, *Optical Properties of Metal Clusters* (Springer-Verlag, Berlin, Germany, 1995).
[2] R. Elghanian, J. J. Storhoff, R. C. Mucic, R. L. Letsinger, and C. A. Mirkin, "Selective colorimetric detection of polynucleotides based on the distance-dependent optical properties of gold nanoparticles," Science **277**, 1078-1081 (1997).

[3] S. Nie and S. R. Emory, "Probing single molecules and single nanoparticles by surface-enhanced Raman scattering," Science **275**, 1102-1106 (1997).
[4] K. L. Kelly, E. Coronado, L. L. Zhao, and G. C. Schatz, "The optical properties of metal nanoparticles: The influence of size, shape, and dielectric environment," J. Phys. Chem. B **107**, 668-677 (2003).
[5] P. K. Jain, X. Huang, I. H. El-Sayed, and M. A. El-Sayed, "Noble metals on the nanoscale: Optical and photothermal properties and some applications in imaging, sensing, biology, and medicine," Acc. Chem. Res. **41**, 1578-1586 (2008).
[6] Q. H. Wei, K. H. Su, S. Durant, and X. Zhang, "Plasmon resonance of finite one-dimensional Au nanoparticle chains," Nano Lett. **4**, 1067-1071 (2004).
[7] Z. Zhang, A. Weber-Bargioni, S. W. Wu, S. Dhuey, S. Carbini, and P. J. Schuck, "Manipulating nanoscale light fields with the asymmetric bowtie nano-colorsorter," Nano Lett. **9**, 4505-4509 (2009).
[8] P. K. Jain and M. A. El-Sayed, "Plasmonic coupling in noble metal nanostructures," Chem. Phys. Lett. **487**, 153-164 (2010).
[9] K. Parshant and M. A. El-Sayed, "Noble metal nanoparticle pairs: Effect of medium for enhanced nanosensing," Nano Lett. **8**, 4347-4352 (2008).
[10] P. K. Jain, W. Huang, and M. A. El-Sayed, "On the universal scaling behavior of distance decay of plasmon coupling in metal nanoparticle pairs: A plasmon ruler equation," Nano Lett. **7**, 2080-2088 (2007).
[11] J. B. Lassiter, J. Azipurua, L. I. Hernandez, D. W. Brandl, I. Romero, S. Lal, J. H. Hafner, P. Nordlander, and N. J. Halas, "Close encounters between two nanoshells," Nano Lett. **8**, 1212-1218 (2008).
[12] H. Tamaru, H. Kuwata, H. T. Miyazaki, and K. Miyano, "Resonant light scattering form individual Ag nanoparticles and particle pairs," Appl. Phys. Lett. **80**, 1826-1828 (2002).
[13] A. Ahmadivand, M. Karabiyik, and N. Pala, "Fano-like resonances in split concentric nanoshell dimers in designing negative-index metamaterials for biological-chemical sensing and spectroscopic purposes," Appl. Spectrosc. **69**, 563-573 (2015).
[14] S. Sheikholeslami, Y. W. Jun, P. K. Jain, and A. P. Alivisatos, "Coupling of optical resonances in a compositionally asymmetric plasmonic nanoparticle dimer," Nano Lett. **10**, 2655-2660 (2010).
[15] E. Prodan, C. Radloff, N. J. Halas, and P. Nordlander, "A hybridization model for the plasmon resonance of complex nanostructures," Science **302**, 419-422 (2003).
[16] P. K. Jain, S. Eustis, and M. A. El-Sayed, "Plasmon coupling in nanorod assemblies: Optical absorption, discrete dipole approximation simulation, and extinction coupling model," J. Phys. Chem. B **110**, 18243-18253 (2006).
[17] T. J. Antosiewicz and S. Peter Apell, "Optical enhancement of plasmonic activity of catalytic metal nanoparticles," RSC Adv. **5**, 6378-6384 (2015).
[18] L. S. Slaughter, Y. Wu, B. A. Willingham, P. Nordlander, and S. Link, "Effect of symmetry breaking and conductive contact on the plasmon coupling in gold nanorod dimers," ACS Nano **4**, 4657-4666 (2010).
[19] B. Luk'yanchuk, N. I. Zheludev, S. A. Maier, N. J. Halas, P. Nordlander, H. Giessen, and C. T. Chong, "The Fano resonances in plasmonic nanostructures and metamaterials," Nat. Mater. **9**, 707-715 (2010).
[20] K. C. Woo, L. Shao, H. Chen, Y. Liang, J. Wang, and H. –Q. Lin, "Universal scaling and Fano resonance in the plasmon coupling between gold nanorods," ACS Nano **5**, 5976-5986 (2011).
[21] Y, -I. Xu, "Electromagnetic scattering by an aggregate of spheres," Appl. Opt. **34**, 4573-4588 (1995).
[22] P. Zhang, J. Feist, A. Rubio, P. García-González, and F. J. García-Vidal, "Ab ignition nanoplasmonics: The impact of atomic structure," Phys. Rev. B **90**, 161407(R) (2014).
[23] B. Willinghaam, D. W. Brandl, and P. Nordlander, "Plasmon hybridization in nanorod dimers," Appl. Phys. B **93**, 209-216 (2008).
[24] D. E. Gomez, Z. Q. Teo, M. Altissimo, T. J. Davis, S. Earl, and A. Roberts, "The dark side of plasmonics," Nano Lett. **13**, 3722-3728 (2013).
[25] G. Fletcher, M. D. Arnold, T. Pedersen, V. J. Keast, and M. B. Cortie, "Multipolar and dark-mode plasmon resonances on drilled silver nano-triangles," Opt. Express **23**, 18002-18013 (2015).
[26] M. A. Taubenblatt and T. K. Tran, "Calculating of light scattering from particles and structures on a surface by the coupled-dipole method," J. Opt. Soc. Am. A **10**, 912-919 (1993).
[27] B. T. Draine and P. J. Flatau, "Discrete-dipole approximation for scattering calculations," J. Opt. Soc. Am. A **11**, 1491-1499 (1994).
[28] C. F. Bohren and D. R. Huffman, *Absorption and scattering of light by small particles* (Wiley, Germany, Berlin, 1983).
[29] A. J. Logsdail, *Computational characterization of gold nanocluster structures* (Springer, Switzerland, 2013).
[30] C. Radloff and N. J. Halas, "Plasmonic properties of concentric nanoshells," Nano Lett. **4**, 1323-1327 (2004).
[31] O. Pena-Rodriguez and U. Pal, "Geometrical tunability of linear optical response of silica-gold double concentric nanoshells," J. Phys. Chem. C **114**, 4414-4417 (2010).
[32] A. Ahmadivand and N. Pala, "Localization, hybridization, and coupling of plasmon resonances in an aluminum nanomatryushka," Plasmonics **10**, 809-817 (2015).
[33] E. D. Palik, *Handbook of optical constants of solids*, 2nd ed. (Academic Press, San Diego, 1991).
[34] R. D. Averitt, S. L. Westcott, and N. J. Halas, "Linear optical properties of gold nanoshells," J. Opt. Soc. Am. B **16**, 1824-1832 (1999).
[35] A. Ahmadivand and S. Golmohammadi, "Comprehensive investigation of noble metal nanoparticles shape, size, and material on the optical response of optimal plasmonic Y-splitter waveguides," Opt. Commun. **310**, 1-14 (2014).
[36] G. Bachelier, I. Russier-Antoine, E. Benichou, C. Jonin, N. Del Fatti, F. Vallee, and P. F. Brevet, "Fano profiles induced by near-field coupling in heterogenous dimers of gold and silver nanoparticles," Phys. Rev. Lett. **101**, 197401 (2008).